Sharp asymmetric line shapes in side-coupled waveguide-cavity systems

Shanhui Fan[a)]
Department of Electrical Engineering, Stanford University, Stanford, California 94305

(Received 1 October 2001; accepted for publication 29 November 2001)

We show that, for an optical microcavity side coupled with a waveguide, sharp, and asymmetric line shapes can be created in the response function by placing two partially reflecting elements into the waveguides. In such a system, the transmission coefficient varies from 0% to 100% in a frequency range narrower than the full width of the resonance itself. We numerically demonstrate this effect by simulating the propagation of electromagnetic waves in a photonic crystal. © *2002 American Institute of Physics.* [DOI: 10.1063/1.1448174]

Optical microcavity structures are of great current interests for device applications. These structures can exhibit high quality factors, and small modal volumes approaching $(\lambda/2n)^3$. An intriguing potential application for such cavity structures is their use in optical modulations and switching.[1] The on/off switching functionality, for example, can be realized by shifting the resonant frequency either toward or away from the signal frequency. To achieve a large on/off contrast ratio, however, the required frequency shift tends to be much larger than the width of a single resonance.

In this letter, we introduce a geometry that significantly reduces the frequency shift required for on/off switching in a microcavity structure. The basic geometry, as shown in Fig. 1(a), consists of a waveguide side coupled with a single-mode cavity. This geometry typically behaves as a narrow-band reflector with a symmetric Lorentzian reflectivity line shape.[2] Here, however, we intentionally incorporate two partially reflecting elements into the waveguide [Fig. 1(b)]. We show that these elements can create sharp and asymmetric response line shapes. Such line shapes may allow the tuning of the system between zero and complete transmission, with a frequency shift that is significantly narrower than the full width of the resonance itself.

To start, let us first briefly review the properties of the basic geometry as shown in Fig. 1(a). Quantitatively, the scattering property of this system for incident waves at a frequency ω can be described using a transfer matrix T_c, as[2,3]

$$\begin{bmatrix} b_2 \\ a_2 \end{bmatrix} \equiv T_c \begin{bmatrix} a_1 \\ b_1 \end{bmatrix} = \begin{bmatrix} 1-\dfrac{i\gamma}{\omega-\omega_0} & \dfrac{-i\gamma}{\omega-\omega_0} \\ \dfrac{i\gamma}{\omega-\omega_0} & 1+\dfrac{i\gamma}{\omega-\omega_0} \end{bmatrix} \begin{bmatrix} a_1 \\ b_1 \end{bmatrix}, \tag{1}$$

where ω_0 and γ are the center frequency and the width of the resonance. The transfer matrix relates the incoming and outgoing wave amplitudes a_1 and b_1 on one side of the cavity, to the outgoing and incoming wave amplitudes b_2 and a_2 on the other side. From Eq. (1), the reflection coefficient $R(\omega)$ is determined as

$$R(\omega) = \frac{\gamma^2}{(\omega-\omega_0)^2+\gamma^2}. \tag{2}$$

The presence of the partially reflecting elements, as shown in Fig. 1(b), significantly perturbs the phase of the wave amplitudes that are directly transmitted through the waveguide, and therefore leads to complex interference phenomena. Quantitatively, the response function of the system as shown in Fig. 1(b) can be calculated by combining the transfer matrix of each individual element in the system. For the partially reflecting element, the transfer matrix T_p is determined as[4]

$$T_p = \frac{1}{i\sqrt{1-r^2}} \begin{bmatrix} -1 & -r \\ r & 1 \end{bmatrix}, \tag{3}$$

where r is the amplitude reflectivity of the element. Therefore, the transfer matrix T_s for the entire system is determined by

$$\begin{aligned} T_s = &-\frac{1}{1-r^2} \begin{bmatrix} -1 & -r \\ r & 1 \end{bmatrix} \begin{bmatrix} e^{i\delta} & 0 \\ 0 & e^{-i\delta} \end{bmatrix} \\ &\times \begin{bmatrix} 1-\dfrac{i\gamma}{\omega-\omega_0} & \dfrac{-i\gamma}{\omega-\omega_0} \\ \dfrac{i\gamma}{\omega-\omega_0} & 1+\dfrac{i\gamma}{\omega-\omega_0} \end{bmatrix} \begin{bmatrix} e^{i\delta} & 0 \\ 0 & e^{-i\delta} \end{bmatrix} \\ &\times \begin{bmatrix} -1 & -r \\ r & 1 \end{bmatrix}, \end{aligned} \tag{4}$$

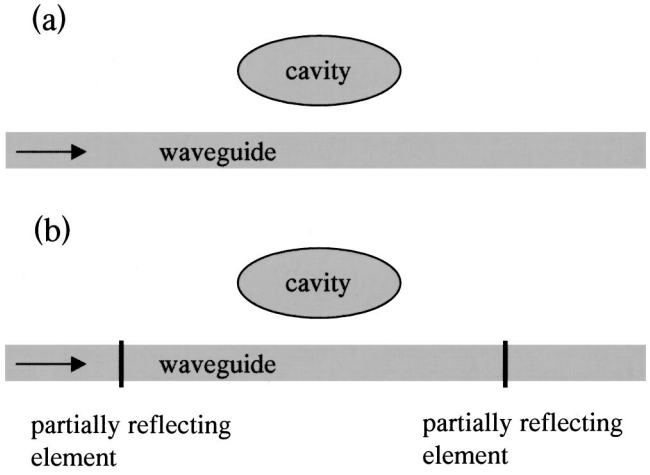

FIG. 1. Optical systems consisting of a waveguide side coupled to a single-mode cavity. (a) The basic geometry, as analyzed in Refs. 2 and 3; (b) A geometry where two partially reflecting elements are placed in the waveguide. The arrow indicates the direction of the input light.

a)Electronic mail: shanhui@stanford.edu

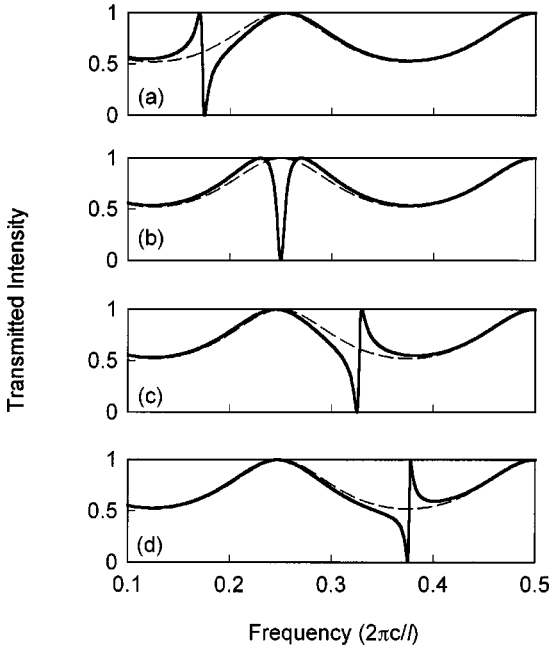

FIG. 2. The solid lines are theoretical transmission spectra through the optical system as shown in Figure 1(b). The spectra are calculated from Eq. (5). We plot the frequencies in the unit of $(2\pi c/l)$, where $2l$ is the distance between the two reflecting elements. The reflecting element has a reflection coefficient $r=0.4$. The width of the resonance is $0.002(2\pi c/l)$. The resonant frequencies of the cavity are taken to be: (a) $0.175(2\pi c/l)$, (b) $0.25(2\pi c/l)$, (c) $0.325(2\pi c/l)$, and (d) $0.375(2\pi c/l)$. The dashed lines represent the transmission spectrum through the two reflecting elements, without the presence of the cavity.

where $\delta \equiv \omega l/c$ is the phase shift that the waveguide mode acquires as it propagates, with a phase velocity c, from the partially reflecting element to the cavity.

From Eq. (4), the amplitude transmissivity t_s is determined as

$$t_s = \frac{1}{T_{s,22}} = \frac{(r^2-1)e^{2i\delta}(\omega-\omega_0)}{-e^{4i\delta}r^2(\omega-\omega_0-i\gamma)-2e^{2i\delta}(i\gamma)r+\omega-\omega_0+i\gamma}. \quad (5)$$

To explore the physical phenomena encapsulated in Eq. (5), in Fig. 2 we plot the intensity transmission spectra that are determined from Eq. (5). For concreteness, we assume $r=0.4$ and $\gamma=0.002\cdot(2\pi c/l)$, and vary the resonant frequency ω_0. As a comparison, we also plot in Fig. 2 as dashed lines the transmission spectra for the same system without the cavity. The dashed line shows the typical Fabry–Pérot oscillations with a maximum occurring at $\omega=0.25\cdot(2\pi c/l)$.

Examining Fig. 2 we note that the spectra consist of resonant features superimposed upon a background defined by the Fabry–Pérot oscillations. The shapes of the resonant features depend critically on the relative positions of the resonant frequency in relation to the background. In particular, when the resonant frequency coincides with a maximum of the Fabry–Pérot oscillations, the transmission exhibits a *symmetric* Lorentzian-like line shape, as can been seen in the case of Fig. 2(b) where $\omega_0=0.25\times(2\pi c/l)$. The structure behaves as a narrow-band reflector.

For most choices of resonant frequencies, on the other hand, the spectra display a distinct asymmetric line shape. In the immediate vicinity of the resonant frequency ω_0, the transmission coefficient varies sharply from 0% to 100%. From Eq. (5), one can determine that the transmission vanishes at a frequency $\omega_r=\omega_0$, while the transmission reaches 100% at a frequency ω_t calculated as

$$\frac{\omega_t-\omega_0}{\gamma} = -\frac{1+r^2-2r\cos(2\delta)}{2r\sin(2\delta)}. \quad (6)$$

In the limit where the width of the resonance is narrow, the phase shift δ varies slowly across the bandwidth of the resonance. We can therefore directly determine ω_t using Eq. (6) by approximating $\delta(\omega)$ with $\delta(\omega=\omega_0)$.

The difference between ω_t and ω_0, as calculated from Eq. (6), determines the frequency shift needed to switch the system from complete reflection to complete transmission. Assuming, for example, that $r=0.4$ and $2\delta=(2n+1/2)\pi$, the shift can then be as small as 1.45γ. In comparison, in order to achieve an on/off contrast ratio of 30 dB in a single-mode microcavity structure with a Lorentzian response function, the required frequency shift exceeds 31γ. Moreover, as we note from Fig. 2, the asymmetric line shapes persist with wide ranges of parameters. The occurrence of this phenomena should therefore be robust against fabrication inaccuracies.

To realize the results of the analytic theory, we consider the propagation of an electromagnetic wave in a photonic crystal structure as shown in Fig. 3. The crystal is made up of a square lattice of high-index dielectric rods with a radius of $0.20a$, where a is the lattice constant. In the crystal, a waveguide is formed by removing a row of dielectric rods,[5] and a cavity is created by reducing the radius of a single cylinder to $0.10a$. The cavity is placed at a distance $2a$ away from the center of the waveguide. Such a cavity supports a localized monopole state which is singly degenerate.[6] Within the waveguide, we introduce two small cylinders, each with a radius $0.05a$, to provide the partial reflection for waveguide modes. All the cylinders in the crystal, including the smaller ones, have a dielectric constant of 11.56, which corresponds to the dielectric constant of Si at optical wavelengths.

We simulate the response of the structure shown in Fig. 3 using a finite-difference time-domain scheme[7] with the perfectly matched layer boundary conditions.[8] At the entrances to the photonic crystal waveguide, structures consisting of a defect in a distributed Bragg mirror are placed to reduce reflection.[9] A pulse is excited by a monopole source at one end of the waveguide. The transmission coefficients are then calculated by Fourier transforming the amplitude of the fields at the other end, and are shown as a solid line in Fig. 4. In comparison, we also show in Fig. 4 the transmission spectra for the same structure, except without the two small cylinders in the waveguide.

Without the two smaller cylinders in the waveguide (Fig. 4, the dashed line), the transmission spectrum approximates a Lorentzian, with the resonant frequency $\omega_0=0.3600\cdot(2\pi c/a)$, and the full-width at half minimum $2\gamma=0.0024\cdot(2\pi c/a)$. At the resonant frequency, the transmission drops to 0%, and the structure behaves as a narrowband reflector. In contrast, the two smaller cylinders in the waveguide gen-

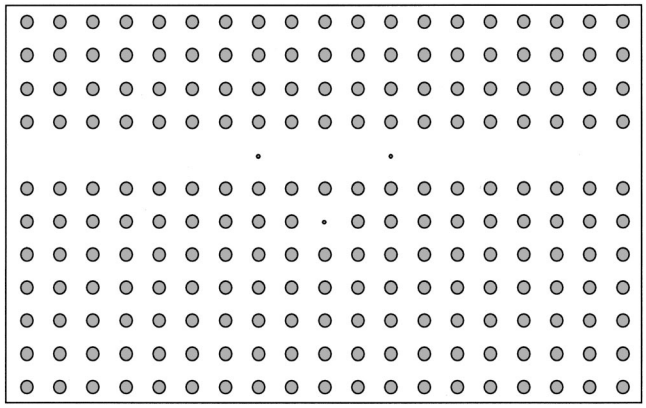

FIG. 3. A photonic crystal structure. The crystal consists of a square lattice of rods with a dielectric constant of 11.56 and a radius of $0.2a$. A line defect is formed by removing a single row of rods. Within the line defect there are two smaller rods with a radius of $0.05a$. A point defect, created by reducing the radius of a single rod to $0.10a$. is placed $2a$ away from the center of the line defect.

erate a sharp and asymmetric line shape (Fig. 4, the solid line). The structure remains completely reflecting at ω_0. However, as the frequency increases from ω_0, the transmission coefficient increases rapidly and reaches a maximum that exceeds 99% at a frequency $\omega_t = 0.3613 \cdot (2\pi c/a)$. The difference between ω_t and ω_0 of $0.0013 \cdot (2\pi c/a)$ is far smaller than the full width at half minimum of the cavity resonance. All the features completely agree with the analytic theory.

The steady state field distributions at the two frequencies ω_t and ω_0 are shown in Fig. 5. At $\omega = \omega_0$, the field is completely reflected [Fig. 5(a)], while at $\omega = \omega_t$, the field remains transmitted in the waveguide [Fig. 5(b)]. A unique feature here is the existence of significant optical power within the cavity for *both* of these two states. This is further evidence that both frequencies fall within the line shape of the resonance.

As closing remarks, we note that no detailed tuning of either the resonant frequency or the coupling between the cavity and the waveguide is required to achieve the asymmetric line shapes. Also, since the reflectivity of the partially reflecting elements need not be large, the underlying physics

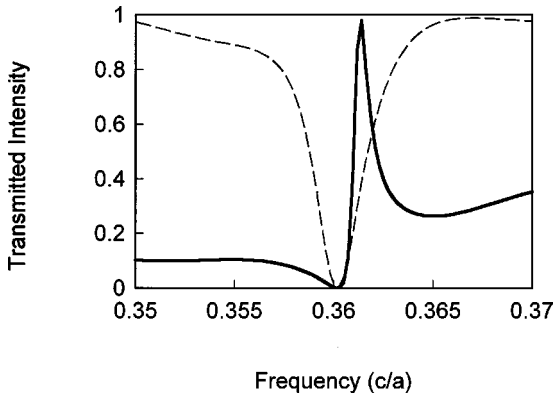

FIG. 4. The solid line is the transmission spectra through the structure as shown in Fig. 3. The dashed line is the transmission spectra for the same structure, without the two smaller rods in the line defect.

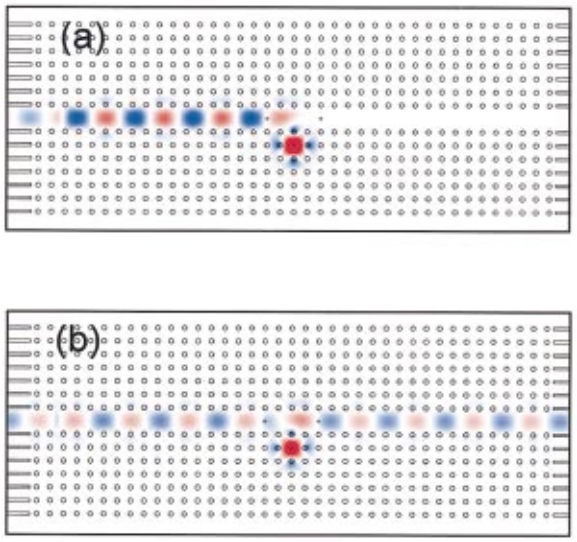

FIG. 5. (Color) Steady-state electric field distribution in the structure as shown in Fig. 3, for the incident frequencies at: (a) $\omega = 0.3600(2\pi c/a)$ and (b) $\omega = 0.3613(2\pi c/a)$. The colors red and blue represent large positive and negative fields, respectively.

here differs from typical coupled-cavity systems, and resembles instead the Fano resonances involving interference between a continuum and a discrete level.[10] Finally, for structures with inherent radiation losses from the cavity, such as photonic crystal slabs,[11] the criteria for observing this effect is that the decay of the cavity mode into the waveguide dominates over the inherent loss of the cavity. Since point defect modes in photonic crystal slab structures may have radiation Q exceeding 15 000,[12] the effect reported here may allow the construction of devices that can switch from complete transmission to complete reflection with a fractional change of the index approaching 10^{-4}. Achieving such an effect may be important for lowering the power threshold in optical bistable devices, and for sensing applications.

The author acknowledges useful discussions from A. Siegman, S. Harris, and D. Miller. The simulations were performed at the NSF San Diego Supercomputing Center (SDSC).

[1] P. R. Villeneuve, D. S. Abrams, S. Fan, and J. D. Joannopoulos, Opt. Lett. **21**, 2017 (1996).
[2] H. A. Haus and Y. Lai, J. Lightwave Technol. **9**, 754 (1991).
[3] Y. Xu, Y. Li, R. K. Lee, and A. Yariv, Phys. Rev. E **62**, 7389 (2000).
[4] H. A. Haus, *Waves and Fields in Optoelectronics* (Prentice–Hall, New York, 1984).
[5] J. D. Joannopoulos, R. D. Meade, and J. N. Winn, *Photonic Crystals* (Princeton University Press, Princeton, NJ, 1995).
[6] P. R. Villeneuve, S. Fan, and J. D. Joannopoulos, Phys. Rev. B **54**, 7837 (1996).
[7] For a review on finite difference time domain methods, see A. Taflove and S. C. Hagness, *Computational Electrodynamics: The Finite-Difference Time-Domain Method* (Artech House, Boston, 2000).
[8] J. P. Berenger, J. Comput. Phys. **114**, 185 (1994).
[9] A. Mekis, S. Fan, and J. D. Joannopoulos, IEEE Microwave Guid. Wave Lett. **9**, 502 (1999).
[10] U. Fano, Phys. Rev. **124**, 1866 (1961).
[11] S. G. Johnson, S. Fan, P. R. Villeneuve, J. D. Joannopoulos, and L. A. Kolodziesjski, Phys. Rev. B **60**, 5751 (1999).
[12] O. Painter, T. Vuckovic, and A. Scherer, J. Opt. Soc. Am. B **16**, 275 (1999).